Different composting modes shape specific community structure of ammonia oxidizer and denitrifier correlated with N_2O emissions

Submitted to the NAXOS 2018
6th International Conference on Sustainable Solid Waste Management
May 2018

Tao Jiang[a,b], Jiali Chang[a*], Juan Yang[a], Feng Yang[a], Xuguang Ma[a], Zhigang Yi[a], Qiong Tang[a], Wenhai Luo[b], Guoxue Li[b*]

[a]*College of Chemistry, Leshan Normal University, Leshan 614004, China*
[b]*College of Resources and Environment Sciences, China Agricultural University, Beijing 100193, China*

[*] Corresponding author. *E-mail address:*jialiyangfeng@163.com (J. Chang)
[*] Corresponding author. *E-mail address:* composting@163.com (G. Li)

Abstract

This study was performed to investigate the variations of microbial community structures, contributing to N_2O emission, during pig manure composting under different modes (including forced aeration, turn windrow and static pile). Terminal restriction fragment length polymorphism (T-RFLP) and clone sequencing targeted bacterial *amoA* and *nirK* genes were adopted to clarify the differential responses of ammonia oxidizing bacteria (AOB) and *nirK*-type denitrifiers. Results showed the accumulative N_2O emission rate of forced aeration treatment was 2.4% of initial nitrogen, which was 2.2 and 1.8 times higher than that of turn windrow and static pile, respectively. Such distinct N_2O emissions pattern was closely correlated with the variation of community structures of AOB and *nirK*-type denitrifiers. Co-existence of *Nitrosomonas spp.* with 45 bp T-RF of *amoA* gene and denitrifier with 189 bp T-RF of *nirK* gene could contribute to the substantial emissions of N_2O in forced aeration mode. This study provides unique insights to further understand the mechanism of N_2O emissions among different composting modes.

Keywords: composting; nitrous oxide; amoA; nirK; ammonia oxidizing bacteria; denitrifier.

1. Introduction

Nitrous oxide (N_2O) is an important greenhouse gas (GHG) and vital participant in ozone deterioration [1,2]. Composting is one of the significant sources of N_2O production, which accounts for approximately 30-50% of the annual global N_2O emissions from agriculture [3,4].

N_2O can be formed as a byproduct of nitrification and an intermediate product of denitrification [5]. Genes encoding the key enzymes of the above process were generally quantified to evaluate N_2O emissions through quantitative real-time polymerase chain reaction (qPCR) technology [3-9]. For instance, *amoA* and *nosZ* genes respectively encoding alpha subunit of ammonia mono-oxygenase and N_2O reductase were utilized to determine the contribution of nitrifying and denitrifying pathways to N_2O emissions [6]. The quantities of *nirK* and *nirS* gene encoding two types of nitrite reductase were mostly utilized to indicate N_2O production potential [7,8]. Recently, the *nosZ*/(*nirK* + *nirS*) ratio had been declared to act as good indicator for predicting N_2O emissions [9].

Composting system is made of complex raw materials including animal manure and straw, providing ideal circumstance for diverse microorganism to colonize. Nitrifier and denitrifier were key actors participating in N_2O emissions during composting [10]. Even though most of studies correlated N_2O emissions with the quantities of nitrifying and denitrifying genes, the functional microbial community structure had been highlighted as the vital regulator of the ecosystem [11]. It was recently demonstrated that community structure of denitrifiers based on *nirK* gene was closely related with nitrate content of soil amended with biochar [12]. Thereupon, the community structure of nitrifiers and denitrifiers should also be considered when evaluating the N_2O emissions during composting.

This study mainly focused on investigating functional microbial responses in terms of community structures to different composting modes for N_2O emissions. Three composting modes were evaluated, namely forced aeration, turn windrow and static pile modes. The relationships among the N_2O production, community structure of AOB and denitrifier, and environmental factors were elucidated.

2. Materials and methods

2.1. Raw materials and composting installation

Pig feces and chopped cornstalks were collected and mixed at a ratio of 7:1 (w/w) as mentioned previously [13]. The compositions of raw materials and their mixture were shown in Table 1. Rotting boxes (1.08×0.8×1.4 m) were used to simulate central parts of composting piles in practice. The details of instrument were shown is Fig.1.

Table1 The compositions of raw materials and mixture

	TOC	TKN	NH_4^+-N	NO_3^--N	Moisture content	C/N
		($g \cdot kg^{-1}$ DM)		($mg \cdot kg^{-1}$ DM)	(%)	
Pig feces	251.3±10.3	30.4±0.2	5.8±0.3	68.6±5.9	70.2±3.6	8.4±0.5
Corn stalk	419.0±13.6	9.6±0.1	-	-	9.3+0.1	42.3±3.5
Mixture	298.1±11.2	21.8±0.2	3.5±0.1	41.5±3.7	62.6±2.3	13.7±0.6

TOC: total organic carbon; TN: total nitrogen; DM: dry matter.

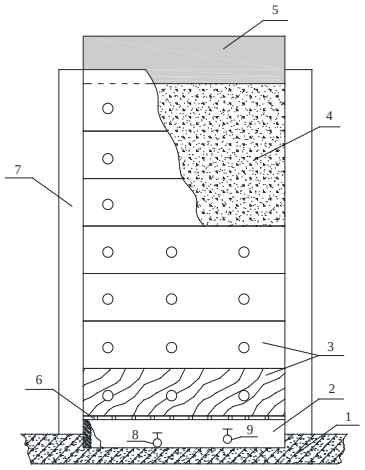

Fig.1 Sketch map of compost rotting box. 1: concrete floor; 2: aeration and leachate cavum; 3: wooden boards with sampling holes; 4: compost materials; 5: removable vented chamber; 6: bottom board with aeration holes; 7: concrete side wall. 8: valve for leachate; 9: valve for forced aeration

2.2. Experimental design and composting methods

Three different composting modes (static pile, turning windrow, forced aeration) were conducted. The static pile was set without turning and forced aeration. Both turning windrow and forced aeration treatment were turned weekly. The aeration rate of forced aeration treatment was $0.25 L \cdot kgDM^{-1} \cdot min^{-1}$.

All piles were composted for 77 days. During each turning, samples were separately taken at the top, middle and bottom layers, and five samples were evenly taken at each layer. Certain amount of samples was stored at -80°C for microbial analysis. Some parties of samples were stored at - 4°C as fresh samples. The remaining samples were air-dried, ground, passed through a 0.1 mm sieve and then stored for further analysis.

2.3. Physicochemical analysis

N_2O and NH_3 emission rates and concentrations in different layers of the compost piles were measured daily during the first week, and then 3 to 4 times per week thereafter. N_2O was analyzed by gas chromatograph equipped with electron capture detectors (Agilent 7890A, USA). NH_3 was absorbed by 2% boric acid (m/m) and then titrated using 0.05 mole L^{-1} H_2SO_4. The O_2 content at different layers of

compost piles were measured by an O_2 detector (Umwelt-Electronic CM-37, Germany).

Inorganic nitrogen (NH_4^+-N, NO_3^--N, NO_2^--N) was extracted with 2 mole L^{-1} KCl (1:20) and analyzed by ion chromatography (Thermo Scientific ICS-900, USA). Total organic carbon (TOC) and total nitrogen (TN) contents were measured using an Element analyzer (Elementarvario MACRO cube, Germany).

2.4. Microbial analysis

2.4.1 DNA extraction and Polymerase chain reaction (PCR)

DNA was extracted using the Fast-DNA Spin Kit for Soil (MP Biomedicals, Santa Ana, CA). DNA concentrations and purity were determined via the NanoDrop® Spectrophotometer ND-1000 (Thermo Fisher Scientific, MA, USA).

The primers used for PCR included amoA-1F/amoA-2R, amoA-AF/amoA-AR, nirK1F/nirK5R and nirS1F/nirS6R based on previous studies [14-17], targeting bacterial *amoA*, archaeal *amoA*, *nirK* and *nirS* genes, respectively. The thermal profiles were also referred to the previous studies[14-17], of which *nirK* and *nirS* genes were amplified via nested-PCR. More details could be available in Table 2.

Table 2 Primers & PCR reaction conditions & restriction endonuclease used in this study

Target gene	Primer name	Primer sequence (5'-3')	Thermal profile	No. of cycle	Restriction endonuclease	References
Bac-*amo*A	amoA-1F *	GGGGTTTCTAC TGGTGGT	94°C 45 s, 58°C 45 s, 72°C 45 s.	40	*Msp* I	Horz et al., 2000
	amoA-2R	CCCCTCKGSAA AGCCTTCTTC				
Arc-*amo*A	amoA-AF *	STAATGGTCTG GCTTAGACG	94°C 45 s, 55°C 45 s, 72°C 45 s.	40		Francis et al., 2005 Ying et al., 2010
	amoA-AR	GCGGCCATCCA TCTGTATGT				
*nir*K	nirK-1F	GGMATGGTKCC STGGCA	94°C 30s, 57-52°C 30s (↓0.5°C per cycle), 72°C 40s; 94°C 30s, 55°C 30s, 72°C 40s.	10; 25	*Hae* III	Braker et al., 1998
	nirK-5R *	GCCTCGATCAG RTTRTGG				
*nir*S	nirS-1F *	CCTAYTGGCCG CCRCART	94°C 30s, 56-51°C 30s (↓0.5°C per cycle), 72°C 60s; 94°C 30s, 54°C 30s, 72°C 60s.	10; 25		Braker et al., 1998
	nirS-6R	CGTTGAACTTR CCGGT				

* represents primers labeled with 6-carboxyfluorescein

2.4.2 Terminal restriction fragment length polymorphism (T-RFLP)

For T-RFLP analysis, the forward primer amoA-1F (for bacterial *amoA* gene) and the reverse primer nirK5R (for *nirK* gene) were labeled with 6-carboxyfluorescein. The labeled PCR products were purified

by TIAN Quick Midi Purification Kit (Tiangen, China). Then, they were digested at 37°C for 3.5 h with *MspI* enzyme for bacterial *amoA* gene or with *HaeIII* enzyme (Takara, Japan) for *nirK* gene. The digested products were purified and size-separated by capillary electrophoresis (3730XL GeneticAnalyzer, Applied Biosystems). The relative abundance of individual terminal restriction fragments (T-RFs) was calculated as the percentage of total peak height in a given T-RFLP profile. Only those T-RFs with the relative abundance above 0.5% were considered in analysis.

2.4.3 Cloning and sequencing

To clarify the taxonomic classification of each T-RFs obtained from T-RFLP, clone libraries were constructed from representative samples. After T-RFLP analysis, up-aeration and middle-turn of day59 samples were chosen to construct bacterial *amoA* gene clone libraries. Moreover, origin, up-aeration of day14, up-aeration and up-turn of day59 samples were chosen to construct *nirK* gene clone libraries. PCR amplification used the primers described above without fluorescence labeling. PCR products were purified and ligated into the pMD19-T vector (TaKaRa) according to the manufacturer's instructions. Plasmids were then transformed into *Escherichia coli* cells and the selected positive clones were sequenced using ABI 3730 XL sequencing platform (Majorbio Technology, Shanghai, China). For phylogenetic analysis, nucleotide sequences were translated to deduced amino acid sequences using MEGA5.0. The phylogenetic trees were constructed by 1000-fold bootstrap analysis using the neighbor-joining method with MEGA5.0 program.

The represent *amoA* and *nirK* gene sequences shown in the phylogenetic trees have been deposited in NCBI GenBank under accession numbers MG196062 to MG196082.

2.5. Statistical analysis

The ordination analysis of T-RFLP patterns and its relationship with environmental constrains (NH_4^+-N, NO_3^--N, N_2O and O_2, temperature, pH and ORP) were performed using CANOCO5 (Microcomputer Power, Ithaca, NY).

3. Results and discussion

3.1. Physicochemical dynamics and N_2O emission pattern

As shown in Fig. 2A, the temperature of aeration treatment increased sharply after the experiment was started and rose up to 55°C within 24 h. Without forced aeration, the temperature of the turn windrow and static piles increased tardily, which took 6-7 days to achieve the thermophilic phase. The thermophilic phase of the aeration treatment was approximately 6 weeks. With the exhaustion of easily degradable carbon (Fig. 2C), the temperature decreased gradually, reaching to the atmospheric level after the 7^{th} week. The forced aeration accelerated the composting process by shortening the thermophilic phase [18,19]. At

the end of the experiment, the temperature of static pile was still around 50°C, indicating the composting process was still going on.

A slight N_2O emission was observed at the beginning of composting for all modes (Fig3A.). This initial emission was also observed in previous studies and could be attributed to the denitrification of background nitrate in pig feces [19,20]. With the loss of initial NO_3^- in raw materials, the N_2O emission decreased to undetectable level within the first 2 days and remained at low level throughout the thermophilic stage.

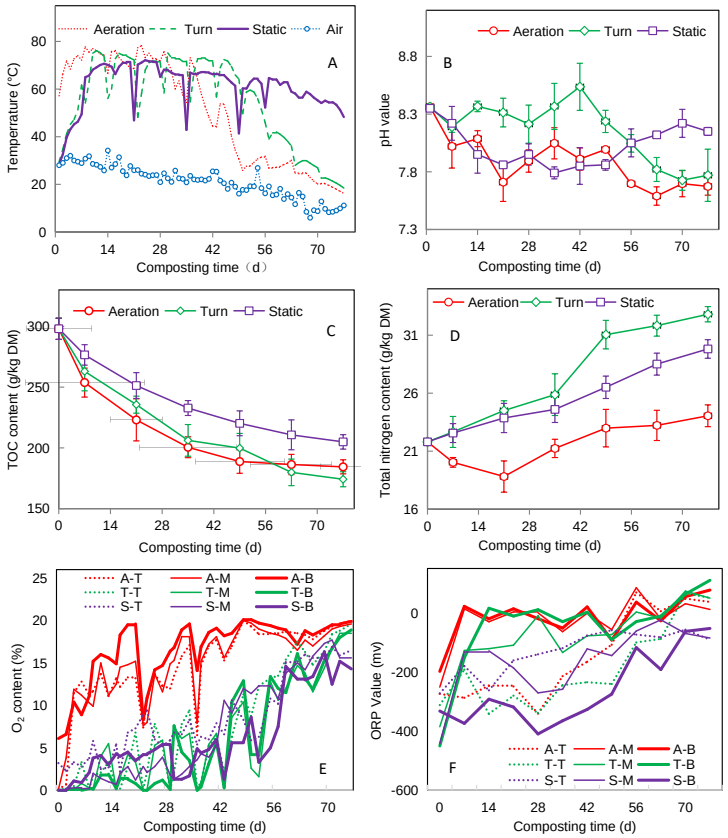

Fig. 2 Physicochemical characteristic evolution during the composting.
A: temperature; B: pH value; C: total organic carbon content; D: total nitrogen content; E: O_2 content in different layer of compost; F: oxidation-reduction potential in different layer of the compost.

The N_2O emission of the static pile began to increase from the 5^{th} week, and the N_2O concentration in the compost pile also increased (Fig. 3A & B). Although the temperature in the pile was still higher than 60 °C, the nitrification process could happen at the surface of the compost pile, where temperature and O_2 content were suitable for nitrobacteria [21]. The nitrate content of static pile also increased during this period (Fig. 3D).

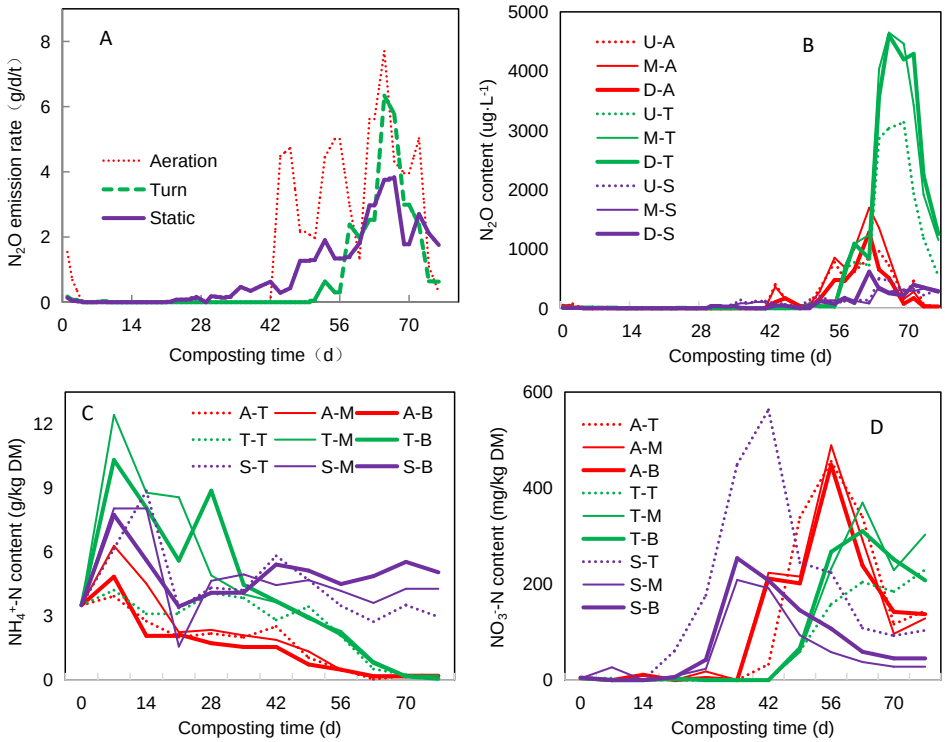

Fig. 3 N_2O surface emission rate pattern (A) and N_2O (B), ammonium (C), nitrate (D) content in the different layer of the compost pile. U-A: up layer of aeration treatment; M-A: middle layer of aeration treatment; D-A: down layer of aeration treatment; U-T: up layer of turn treatment; M-T: middle layer of turn treatment; D-T: down layer of turn treatment; U-S: up layer of static treatment; M-S: middle layer of static treatment; D-S: down layer of static treatment.

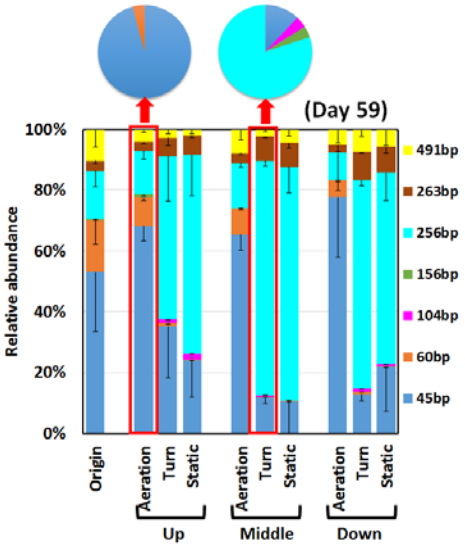

Fig. 4 Succession of ammonia oxidizing bacterial community structure among different treatments based on T-RFLP analysis targeting bacterial *amo*A gene. Samples were collected from origin materials and different layers (include up, middle and down layers) of composting system with different modes (include aeration, turn and static composting mode) at maturity stage (Day59), respectively. Data are means ± standard errors (n = 3). T-RFLP, terminal restriction fragment length polymorphism; bp, base pair. The above pie charts were based on clone sequencing analysis of samples indicated by arrows.

Most N_2O emitted during the maturing stage (Fig. 3A). In this stage, with the exhaust of easily degradable carbon, the TOC content decreased tardily, especially for the aeration treatment (Fig. 2C). It has been reported that the N_2O emission was mostly triggered by nitrification when the easily available carbon sources were depleted [22, 23]. Hence, it was of most concern to further reveal nitrifiers especially ammonia oxidizers' relationship with N_2O emission at maturity stage.

Over the entire composting experiment, the total N_2O emission rate of aeration, turn windrow and static piles was 2.4%, 1.1% and 1.3% of initial nitrogen, respectively. Although the aeration treatment had the highest N_2O emission rate, its N_2O concentration in the compost pile was significantly lower than that of turning treatment (Fig. 3B). The forced aeration not only increased the O_2 supply (Fig. 2E), but also accelerated the air exchange rate in the composting pile and thus increased gas emissions[19].

3.2. Responses of ammonia-oxidizing bacteria (AOB)to composting modes

Generally, the compositions of AOB among samples kept consistent, with the main terminal-restriction fragments (T-RFs) including 45 bp, 60 bp, 104 bp, 156 bp, 256 bp, 263 bp and 491 bp (Fig. 4), all of which were detected in clone libraries and affiliated with the genus of *Nitrosomonas*, except for 263 bp and 491 bp (Fig. 5 & Table 3).

Table 3 Integrated analysis of clone libraries and T-RFLP based on bacterial *amoA* gene

Fragment length (bp)	No. of clones	
	Aeration-Up	Turn-Middle
45	23	3
60	1	-
104	-	1
156	-	1
256	-	20
No. of total clones	24	25

Nevertheless, the community structure of AOB based on the relative abundances of each T-RFs exhibited significant variations under different composting modes. Specifically, 45 bp T-RF was predominant in raw materials and increased from 53% to 77% in aeration mode (Fig. 4). By contrast, 256 bp T-RF overwhelmed 45 bp T-RF and turned to be dominant in turn windrow and static mode (Fig. 4.). Although these T-RFs all belonged to genus *Nitrosomonas*, they located in distinct sub-branches of the phylogenetic tree. In particular, 45 bp T-RF was most closely related with *Nitrosomonas eutropha* (Fig. 5), while 256 bp T-RF belonged to *Nitrosomonas stercoris* that was recently isolated from cattle compost with special characteristic of high ammonium tolerant potential [24]. Hence, it could be deduced that the distinction of AOB community structure was correlated with the content of ammonium among different composting modes (Fig. 3C). Moreover, it seemed that the vertical distribution of AOB was less

influenced by composting modes, with no significant alterations among the up, middle and down layers of the same composting mode (Fig. 4).

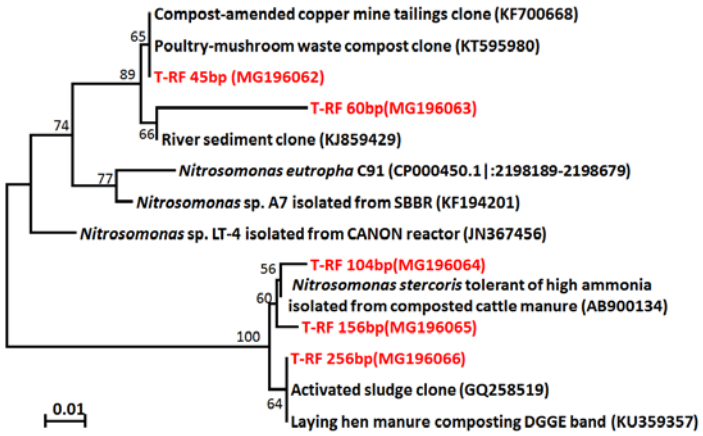

Fig5. Neighbor-joining phylogenetic tree based on aligned partial amino-acid sequences of the *amo*A gene retrieved from two clone libraries (see Fig4. & Table3.). A total of 49 clones were sequenced and clustered into OTUs based on the standard of >97% similarity. Representative sequences of each OTU from this study are shown in the form of T-RF sizes in red color in the tree. The scale bar represents 1% sequence divergence and the GenBank accession numbers of reference sequences are indicated in parentheses.

3.3. Responses of nirK-type denitrifiers to composting modes

Table 4 Integrated analysis of clone libraries and T-RFLP based on *nirK* gene

Fragment length (bp)	No. of clones			
	Origin	Aeraion-Up-14	Aeration-Up-59	Turn-Up-59
60	-	-	-	1
69	5	1	2	8
136	16	11	-	2
155	6	1	-	-
172	1	-	-	-
189	2	-	25	19
228	-	17	-	-
296	-	-	3	-
No. of total clones	30	30	30	30

The succession pattern of *nirK*-type denitrifiers was much more intricate than that of AOB. Notably, the compositions of *nirK*-type denitrifiers varied between thermophilic (Day 14) and maturing stage (Day 59). For instance, 228 bp T-RF was merely detected at up-layers of aeration mode on day 14, yet 189 bp and 296 bp T-RF were generally occurred in maturing stage (Fig. 6), which was also verified by clone sequencing data (Pie chart of Fig. 6 & Table 4). Moreover, 155 bp T-RF predominant in original samples

turned to be less than 1% in up-layers at day 14 and all layers, except for down-layers of static composting mode on day 59.

According to the phylogenetic analysis (Fig. 7), sequences affiliated with 189 bp T-RFs from aeration-up-59 and turn-up-59 samples grouped together, closely related with denitrifier *Castellaniella defragrans* [25]. However, T-RF with the same sizes in original materials located far from the sub-branch, correlated with another denitrifier *Ochrobactrum sp.*. The absolute dominance of 189 bp in both T-RFLP and clone libraries of samples at day 59 demonstrated that denitrifiers belonged to or at least homologous with *C. defragrans* were responsible for the N_2O emission at maturity stage.

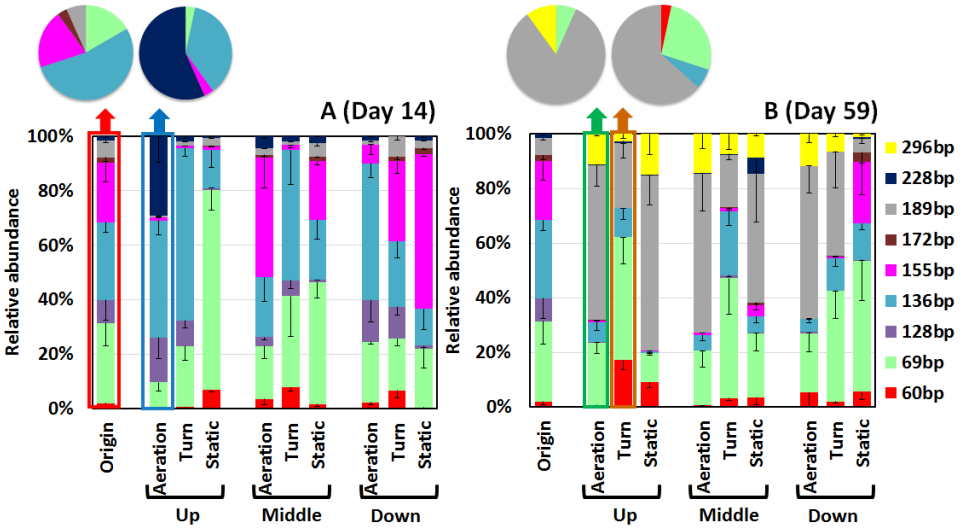

Fig. 6 Succession of denitrifier's community structure among different treatments based on T-RFLP analysis targeting *nir*K gene. Samples were collected from origin materials and different layers (include up, middle and down layers) of composting system with different modes (include aeration, turn and static composting mode) at high-temperature (A, Day14) and maturity stage (B, Day59), respectively. Data are means ± standard errors (n = 3). T-RFLP, terminal restriction fragment length polymorphism; bp, base pair. The above pie charts were based on clone sequencing analysis of samples indicated by arrows.

3.4. Relationships between community structure of functional bacteria and environmental factors

Redundancy analysis (RDA) was adopted to evaluate the relationship between functional bacteria (AOB and *nirK*-type denitrifiers) and environmental factors (including content of NH_4^+-N, NO_3^--N, N_2O and O_2, temperature, pH and ORP) (Fig. 8). For AOB, 45 bp and 60 bp T-RFs were positively correlated with the content of N_2O and O_2, but negatively correlated with pH, temperature and NH_4^+-N (Fig. 8A.). Correspondingly, T-RFs with 256 bp and 263 bp showed the opposite trend. It has been demonstrated that nitrifier denitrification contributed to 90% of the total N_2O produced in the oxidation ditch and *Nitrosomonas* sp. was the dominant AOB causing N_2O emission [26,27]. In this study, it was further

revealed that *Nitrosomonas* spp. with 45 bp and 60 bp T-RFs of *amoA* gene were the potential main N_2O producers at maturity stage of pig manure composting.

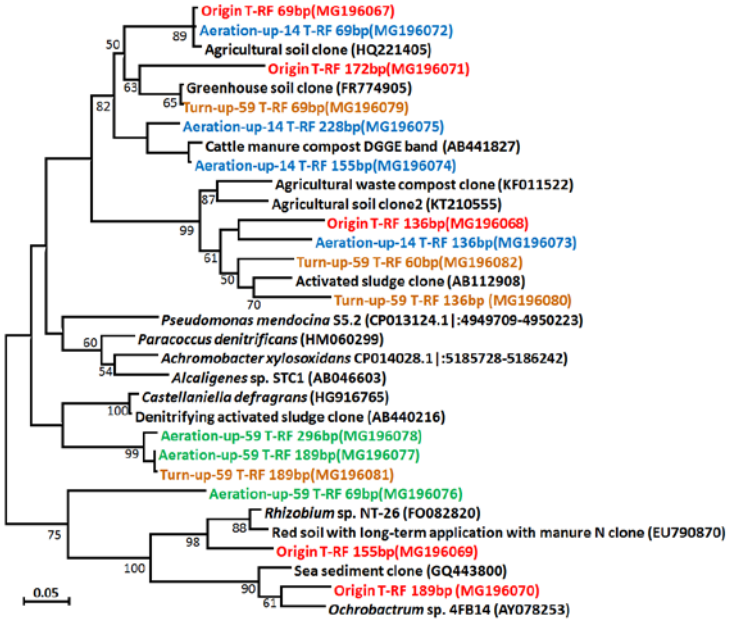

Fig. 7 Neighbor-joining phylogenetic tree based on aligned partial amino-acid sequences of the *nir*K gene retrieved from four clone libraries (see Fig6. & Table4.). A total of 120 clones were sequenced and clustered into OTUs based on the standard of >97% similarity. Representative sequences of each OTU from this study are shown in the form of T-RF sizes with different colors in the tree. The scale bar represents 5% sequence divergence and the GenBank accession numbers of reference sequences are indicated in parentheses.

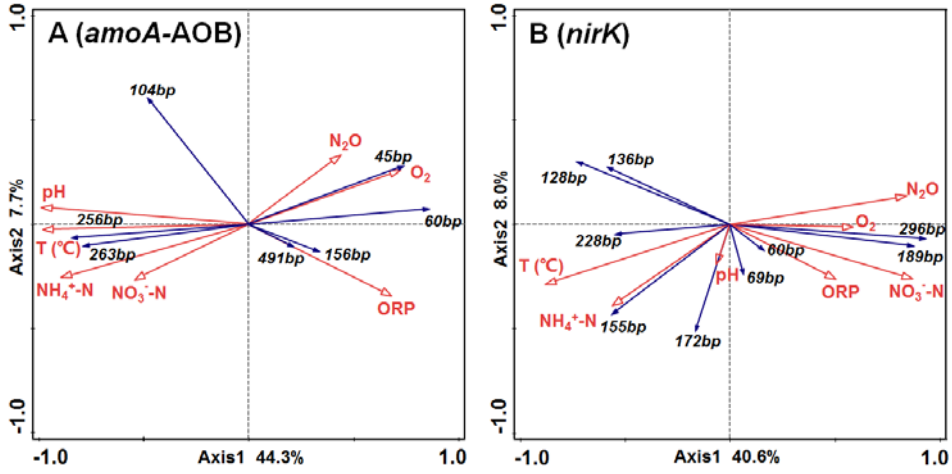

Fig8. Redundancy analysis of T-RFLP profiles generated from bacterial *amo*A gene (A) and *nir*K gene (B) using NH_4^+-N, NO_3^--N, N_2O, O_2, Temperature, pH, ORP as constrains. The eigenvalues of the first and second axis in the two-dimensional ordination diagrams are as follows: Axis 1 = 0.443 and Axis 2 = 0.077 (A) and Axis 1 = 0.406 and Axis 2 = 0.080 (B).

With respect to *nirK*-type denitrifier, 189 bp and 296 bp T-RFs were positively correlated with the content of N_2O and NO_3^--N, but negatively correlated with temperature and NH_4^+-N (Fig. 8B.). ORP, pH and O_2 were less important, indicating the better adaptability of denitrifiers compared with AOB [28].

In summary, variations of physicochemical factors under different composting modes influenced the community structures of AOB and *nirK*-type denitrifiers, which in turn caused the differential N_2O emission patterns. Co-existence of nitrifier with 45 bp T-RF of *amoA* gene and denitrifier with 189 bp T-RF of *nirK* gene could account for the substantial emissions of N_2O in forced aeration composting.

4. Conclusion

In the present study, the accumulative N_2O emission rate of forced aeration treatment was 2.2 and 1.8 times higher than that of turn windrow and static pile, respectively. Composting modes could affect the structure of AOB. The composting mode of turn windrow and static pile increased the abundance of *Nitrosomonas stercoris* (T-RF of 256 bp), which could tolerate high NH_4^+ content. Co-existence of AOB with 45 bp T-RF of *amoA* gene and denitrifier with 189 bp T-RF of *nirK* gene could contribute to the substantial emissions of N_2O in forced aeration mode. Our study provides unique insights to further understand the mechanism of N_2O emissions among different composting modes.

Acknowledgments

This investigation was supported by National Natural Science Foundation of China (No. 41201282), China Agriculture Research System (CARS-39-19), and the National Key Research and Development Program of China (2017YFD0800202).

References

[1] Ravishankara, A.R., Daniel, J.S., Portmann, R.W., 2009. Nitrous oxide (N_2O): the dominant ozone-depleting substance emitted in the 21st century. Science 326, 123-125.

[2] IPCC. 2014. Climate Change 2014: Synthesis Report. IPCC.

[3] Wang, C., Lu, H., Dong, D., Deng, H., Strong, P.J., Wang, H., Wu, W., 2013. Insight into the effects of biochar on manure composting: evidence supporting the relationship between N_2O emission and denitrifying community. Environ. Sci. Technol. 47, 7341-7349.

[4] Li, S., Song, L., Jin, Y., Liu, S., Shen, Q., Zou, J., 2016. Linking N_2O emission from biochar-amended composting process to the abundance of denitrify (nirK and nosZ) bacteria community. AMB Express 6, 37.

[5] Canfield, D.E., Glazer, A.N., Falkowski, P.G., 2010. The evolution and future of earth's nitrogen

cycle. Science 330, 192-196.

[6] Li, W., Sun, Y., Li, G., Liu, Z., Wang, H., Zhang, D., 2017b. Contributions of nitrification and denitrification to N2O emissions from aged refuse bioreactor at different feeding loads of ammonia substrates. Waste Manage. 68, 319-328.

[7] Angnes, G., Nicoloso, R.S., Da, S.M., de Oliveira, P.A., Higarashi, M.M., Mezzari, M.P., Miller, P.R., 2013. Correlating denitrifying catabolic genes with N_2O and N_2 emissions from swine slurry composting. Bioresour. Technol. 140, 368-375.

[8] Li, S., Song, L., Gao, X., Jin, Y., Liu, S., Shen, Q., Zou, J., 2017a. Microbial abundances predict methane and nitrous oxide fluxes from a windrow composting system. Front. Microbiol. 8, 409.

[9] Bian, R., Sun, Y., Li, W., Ma, Q., Chai, X., 2017. Co-composting of municipal solid waste mixed with matured sewage sludge: The relationship between N_2O emissions and denitrifying gene abundance. Chemosphere 189, 581-589.

[10] Maeda, K., Hanajima, D., Toyoda, S., Yoshida, N., Morioka, R., Osada, T., 2011. Microbiology of nitrogen cycle in animal manure compost. Microb. Biotechnol. 4, 700-709.

[11] Cavigelli, M.A., Robertson, G.P., 2000. The functional significance of denitrifier community composition in a terrestrial ecosystem. Ecology 81, 1402-1414.

[12] Liu, Y., Zhu, J., Ye, C., Zhu, P., Ba, Q., Pang, J., Shu, L., 2018. Effects of biochar application on the abundance and community composition of denitrifying bacteria in a reclaimed soil from coal mining subsidence area. Sci. Total Environ. 625, 1218-1224.

[13] Jiang, T., Schuchardt, F., Li, G., Guo, R., Zhao, Y., 2011. Effect of C/N ratio, aeration rate and moisture content on ammonia and greenhouse gas emission during the composting. J. Environ. Sci. (China) 23, 1754-1760.

[14] Braker, G., Fesefeldt, A., Witzel, K.P., 1998. Development of PCR primer systems for amplification of nitrite reductase genes (nirK and nirS) to detect denitrifying bacteria in environmental samples. Appl. Environ. Microbiol. 64, 3769-3775.

[15] Francis, C.A., Roberts, K.J., Beman, J.M., Santoro, A.E., Oakley, B.B., 2005. Ubiquity and diversity of ammonia-oxidizing archaea in water columns and sediments of the ocean. Proc. Natl. Acad. Sci. U. S. A. 102, 14683-14688.

[16] Horz, H.P., Rotthauwe, J.H., Lukow, T., Liesack, W., 2000. Identification of major subgroups of ammonia-oxidizing bacteria in environmental samples by T-RFLP analysis of amoA PCR products. J. Microbiol. Methods 39, 197-204.

[17] Ying, J.Y., Zhang, L.M., He, J.Z., 2010. Putative ammonia-oxidizing bacteria and archaea in an acidic red soil with different land utilization patterns. Environ. Microbiol. Rep. 2, 304-12.

[18] Sundberg, C., Jönsson, H., 2008. Higher pH and faster decomposition in biowaste composting by increased aeration. Waste Manage. 28, 518-526.

[19] Yuan, J., Chadwick, D., Zhang, D., Li, G., Chen, S., Luo, W., Du, L., He, S., Peng, S., 2016. Effects of aeration rate on maturity and gaseous emissions during sewage sludge composting. Waste Manage. 56, 403-410.

[20] Jiang, T., Ma, X., Tang, Q., Yang, J., Li, G., Schuchardt, F., 2016. Combined use of nitrification inhibitor and struvite crystallization to reduce the NH3 and N2O emissions during composting. Bioresour. Technol. 217, 210-218.

[21] Sánchez-Monedero, M.A., Serramiá, N., Civantos, C.G.O., Fernández-Hernández, A., Roig, A., 2010. Greenhouse gas emissions during composting of two-phase olive mill wastes with different agroindustrial by-products. Chemosphere 81, 18-25.

[22] Tsutsui, H., Fujiwara, T., Inoue, D., Ito, R., Matsukawa, K., Funamizu, N., 2015. Relationship between respiratory quotient, nitrification, and nitrous oxide emissions in a forced aerated composting process. Waste Manage. 42, 10-16.

[23] Tsutsui, H., Fujiwara, T., Matsukawa, K., Funamizu, N., 2013. Nitrous oxide emission mechanisms during intermittently aerated composting of cattle manure. Bioresour. Technol. 141, 205-211.

[24] Nakagawa, T., Takahashi, R., 2015. Nitrosomonas stercoris sp. nov., a chemoautotrophic ammonia-oxidizing bacterium tolerant of high ammonium isolated from composted cattle manure. Microbes Environ. 30, 221-227.

[25] Kämpfer, P., Denger, K., Cook, A.M., Lee, S.T., Jäckel, U., Denner, E.B., Busse, H.J., 2006. Castellaniella gen. nov., to accommodate the phylogenetic lineage of Alcaligenes defragrans, and proposal of Castellaniella defragrans gen. nov., comb. nov. and Castellaniella denitrificans sp. nov. Int. J. Syst. Evol. Microbiol. 56, 815-819.

[26] Kong, Q., Liang, S., Zhang, J., Xie, H., Miao, M., Tian, L., 2013. N2O emission in a partial nitrification system: Dynamic emission characteristics and the ammonium-oxidizing bacteria community. Bioresour. Technol. 127, 400-406.

[27] Zheng, M., Tian, Y., Liu, T., Ma, T., Li, L., Li, C., Ahmad, M., Chen, Q., Ni, J., 2015. Minimization of nitrous oxide emission in a pilot-scale oxidation ditch: Generation, spatial variation and microbial interpretation. Bioresour. Technol. 179, 510-517.

[28] Maeda, K., Hanajima, D., Toyoda, S., Yoshida, N., Morioka, R., Osada, T., 2011. Microbiology of nitrogen cycle in animal manure compost. Microb. Biotechnol. 4, 700-709.